

Supplemental Materials

Methods

Study Design

The main objectives of this study were to design a small library of peptide mimetics that directly bind to and inhibit IRF5 activation, test their function *ex vivo* in human healthy and SLE blood, and test *in vivo* in murine models of lupus. For human studies, healthy subjects and SLE patients were randomly selected. SLE patients were evaluated for disease activity using the SLEDAI-2K that assigns individual scores to 24 descriptors; the range is from 0 to 105 (85). Generally, scores ≤ 4 are considered mild disease activity, between 4 and 12 moderate disease activity and > 12 severe disease activity. Because serologic components that may not reflect disease activity are weighted equally with clinical components, each patient was also assigned a Disease Activity Score (DAS) based on clinical disease activity separate from serology. A clinical SLEDAI score refers to the SLEDAI-2K score exclusive of scores for abnormal complement and/or anti-dsDNA values. DAS were derived as follows:

- 0: no disease activity, defined as having normal complement, normal dsDNA titer and a clinical SLEDAI-2K score of 0
- 1: serologically active, clinically stable disease activity, defined as having abnormal serum complement and/or anti-dsDNA titers and a clinical SLEDAI-2K score of 0
- 2: mild disease activity, defined as having a clinical SLEDAI-2K $>0 < 4$
- 3: moderate to severe disease activity, defined as having a clinical SLEDAI-2K ≥ 4 .

For analysis, inactive disease was defined as $DAS \leq 1$ and active disease as $DAS \geq 2$. On the basis of our previous experience using power and statistical analysis for quantifying IRF5 activity in SLE patients (19), a sample size of thirty is sufficient to determine association with disease

activity, SLEDAI and dsDNA antibody titers. For quantifying IRF5 activity in healthy donors, a sample size of eight is sufficient (19). All IRF5 activity measurements were conducted by laboratory staff who were blinded to patient clinical information. Patient dsDNA titers were determined by the clinical laboratory. The assay has a low-end detection limit of <12 and a high-end detection limit of >1000 . We used an arbitrary cut-off of $>12<500$ and >500 to stratify patients. For the mid-range group, titers were from 16-431 with a mean of 153. The >500 group had values that ranged from 517 to >1000 , with a mean of 721. For animal studies, assignment to treatment or control was randomized. Three to six biological replicates (independent experiments) were performed for each animal experiment. All results were analyzed by experimenters who were blinded to experimental groups.

PBMC isolation and IFN- α ELISA

Buffy coats were prepared from fresh blood drawn from consented male and female healthy adults or leukopaks purchased from the New York Blood Center. Blood was diluted 2-fold and subjected to Ficoll density gradient separation (18,19). Isolated PBMC were immediately utilized for experiments. Serum and blood samples from $n = 17$ patients with SLE (male and female) were obtained from the rheumatology clinic at Rutgers New Jersey Medical School in Newark, NJ. Serum and blood samples from $n = 43$ patients with SLE (male and female) were obtained from the Rheumatology clinic at Northwell Health (**Table 1**). Each of the patients fulfilled at least four of the classification criteria for SLE as defined by the American College of Rheumatology (ACR). SLE serum IFN- α levels were determined using the Human IFN- α Serum Sample ELISA Kit following manufacturer instructions (R&D Systems, cat #41110-1).

Synthesis of IRF5 peptide inhibitors

Peptides were synthesized by LifeTein, LLC and purity confirmed by HPLC and mass spectrometry (ST1). The cell permeable sequence alone (PTD) was used as a negative control. Peptides 1-5 (N5-1, N5-2, N5-3, N5-4, N5-5) correspond to N-terminal sequences of IRF5 (Fig. 2A-B); C5-2 corresponds to a C-terminal sequence of IRF5. Individual peptides conjugated to FITC were also synthesized for uptake experiments.

Surface Plasmon Resonance (SPR) Analysis

The Biacore T200 (GE Healthcare, UK) was used for real-time binding interaction studies. Full-length recombinant IRF5 protein (ab173024, Abcam) was immobilized onto a CM5 series chip (GE Healthcare) by diluting to a concentration of 20 $\mu\text{g/mL}$ in 10 mM acetate buffer (pH=5.0). A 1:1 mixture of N-hydroxysuccinimide and N-ethyl-N-(dimethylaminopropyl)carbodiimide was used to activate 2 flow-cells of the CM5 chip. One flow-cell was used as a reference and thus immediately blocked upon activation by 1 M ethanolamine (pH=8.5). The sample flow-cell was injected with the diluted IRF5 at a flow rate of 10 $\mu\text{L/min}$ by manual injection. The IRF5 injection was stopped when the SPR reached ~ 490 RU. For binding of peptides to IRF5, the analytes (peptides) were diluted to 1 μM in 1X PBS+0.05% Tween20 buffer, filtered (0.22 μm) and injected over the IRF5 immobilized chip at a flow rate of 30 $\mu\text{L/min}$ for 60s at 25°C with a dissociation time set for 1 min. Binding experiments were conducted in 1X PBS+0.05% Tween20 as the running buffer; at least 3 independent experiments were performed. For N5-1 and IRF5 kinetics assay, N5-1 was sequentially injected at a flow rate of 20 $\mu\text{L/min}$ for 60s at 25°C with a dissociation time set for 2 minutes, followed by 5s regeneration with 1N NaCl, 10 mM NaOH. N5-1 concentrations were 125, 250, 500, and 1000 nM. The equilibrium dissociation constant (K_D)

was obtained to evaluate the binding affinity by using BIAEvaluation 2.0 software (GE Healthcare) supposing a 1:1 binding ratio. At least 3 independent experiments were performed to determine K_D .

In-cell FRET assay

For intracellular FRET, purified Mo were incubated with 1 μ M FITC-conjugated inhibitor for 1 h, fixed, permeabilized and stained with anti-IRF3 (Abcam #76409), anti-IRF5 (Abcam #124792), or anti-IRF7 (Cell Signaling #4920S) antibodies and TRITC-conjugated secondary antibodies (Abcam). Cell-associated fluorescence was measured on a Biotek Synergy Neo2 (Biotek, VT, USA) at 525 nm upon excitation at 488 nm (E1), at 600 nm after excitation at 540 nm (E2), and at 600 nm after excitation at 488 nm (E3). The transfer of fluorescence was calculated as FRET units as follows:
$$\text{FRET Unit} = (E_{3\text{both}} - E_{3\text{none}}) - ([E_{3\text{TRITC}} - E_{3\text{none}}] \times (E_{2\text{both}}/E_{2\text{TRITC}})) - ([E_{3\text{FITC}} - E_{3\text{none}}] \times [E_{1\text{both}}/E_{1\text{FITC}}])$$
 (86). The different fluorescence values (E) were measured on unlabeled cells (E_{none}), or cells labeled with FITC (E_{FITC}) or TRITC (E_{TRITC}). The photobleaching FRET assay was performed similarly in THP-1 cells (87-88). After pre-incubation with FITC-conjugated inhibitor and staining with anti-IRF3 (Abcam #76409), anti-IRF5 (Abcam #124792 or Bethyl A303-386A), or anti-IRF7 (Cell Signaling #4920S) antibodies, followed by TRITC-conjugated secondary antibodies (Abcam 6718), cells were mounted onto slides. Baseline readings were obtained the first 35 seconds before bleaching, then TRITC was bleached every 15s for 27 cycles on a Zeiss laser scanning confocal microscope 880 with Airyscan (**Supplemental Fig. 4A-C**). Multiple spots of a cell were bleached and these areas were outlined and measured both pre- and post-bleaching. Between 15-20 cells were measured per antibody per independent biological replicate.

Peptide inhibitor titration, uptake and viability

PBMC were treated with 0.025, 0.25, 2.5 and 25 μ M of FITC-conjugated peptide inhibitors (PTD, N5-1 or C5-2) for 2 h. Cells were washed, stained with propidium iodide, and immediately analyzed by flow cytometry for viability and uptake of FITC-conjugated peptides. Similarly, cells were treated over a concentration range and apoptosis examined by Annexin V-SyTox co-staining by flow cytometry. For differential cellular uptake, cells were treated over a dose response (0.25, 2.5, 5, 10 and 25 μ M) or with 10 μ M FITC-conjugated inhibitor, washed, and subsequently stained with anti-CD19-BV510 (BD Biosciences Catalog#: 562847) and anti-CD14-PE (Biolegend Catalog# 301806) antibodies for flow cytometry analysis. For imaging flow cytometry, after surface staining and fixation, cells were stained with DRAQ5 nuclear dye and analyzed by Amnis Imagestream X Mark II (EMD Millipore) for uptake of FITC-peptide.

Imaging Flow Cytometry

Imaging flow was performed as previously described on the Amnis Imagestream (19). Briefly, PBMCs from healthy donors were isolated and treated with inhibitor for 1 h, subsequently stimulated with R848 (500 ng/mL) or 2% SLE serum for 2 h, followed by staining for CD19 and CD14. The SLE patient serum used in the current study was selected after screening for its ability to induce a >3-fold increase in IRF5 nuclear translocation in healthy donor Mo (19). After surface staining, PBMC were fixed overnight in 1% paraformaldehyde and then permeabilized (19). Permeabilized cells were blocked in 5% BSA solution and stained for intracellular IRF5 (Abcam Catalog #: ab193245) or phospho(pSer462)IRF5 and FITC-conjugated secondary antibody (Abcam Catalog #: ab6896). Prior to acquisition, DRAQ5 dye was added at a 1:50 dilution. PBMC from SLE patients were only surface-stained and permeabilized for intracellular IRF5 and DRAQ5

staining. Murine PBMC were stained similarly for intracellular Irf5 (Abcam Catalog #: 181553) (89) and APC-conjugated secondary antibody (BioLegend). Images were acquired on the ImageStream using the 40x objective. Nuclear translocation was quantified in the Amnis IDEAS software suite. Gating strategies are shown in **Supplemental Fig. 1**. Briefly, cells were first filtered through the brightfield area vs. brightfield aspect ratio gate to exclude non-viable and doublet events. Following which a similar gate of the DRAQ5 nuclear channel was used. This added an extra measure of stringency for cell viability. Images were gated on either CD14⁺IRF5⁺, CD19⁺IRF5⁺, or CD123⁺BDCA2⁺IRF5⁺ events, followed by gating on images with a Gradient RMS of greater than 20 on the DRAQ5 channel. This was done to select images with a high level of clarity. Finally, IRF5 nuclear translocation was determined through use of the similarity score feature contrasting IRF5 staining with DRAQ5 staining. A similarity score ≥ 2 was considered a translocation event.

Cell Fractionation

Murine RAW264.7 macrophages were purchased from American Type Culture Collection (ATCC) and maintained as per suggested conditions from ATCC. Human primary Mo were purified using the EasySep Isolation Kit (StemCell Tech, #19359) and then pre-incubated with 2.5 μ M PTD, N5-1 or C5-2 for 1 h before stimulating with PBS or 500 ng/mL R848 for 2 h. RAW264.7 cells were pre-incubated with 0.025 μ M, 0.25 μ M or 2.5 μ M N5-1 or PBS for 1 h before stimulating with PBS or 5 μ g/mL LPS for 2 h. Cells were fractionated according to manufacturer's instruction (Cell Signaling, Cell fractionation kit, # 9038). Following fractionation, lysates were sonicated and boiled. Nuclear fraction was analyzed by Western blot as follows: 30 μ L of lysate was loaded onto a 3-8% NuPAGE® Novex® Tris-Acetate gel (Life Technologies, #EA0378BOX) and

transferred onto a 0.45 µm nitrocellulose membrane (Bio-Rad Laboratories). Membrane was blocked in TBS/0.25% Tween 20 containing 5% BSA for 1 h at room temperature and incubated overnight at 4 °C with anti-IRF5 antibodies (Cell Signaling, #13496) followed by HRP-conjugated secondary antibody (Cell Signaling, α-rabbit #7074S). The nuclear fraction was confirmed using Lamin B1 (Cell Signaling, #15068). The ratio of IRF5/Lamin B1 in the nucleus was determined. Membrane was incubated with Clarity™ ECL Western Blotting Substrate (Bio-Rad Laboratories) and chemiluminescence detected with a ChemiDoc™ MP Imaging System (Bio-Rad Laboratories). The PageRuler™ Plus Prestained Protein Ladder (ThermoFisher Scientific) was used for size reference.

Quantitative Real-Time PCR (qPCR)

RNA was prepared from PBMC by Trizol® isolation, followed by quantitative real-time PCR (qPCR) with primer sets for *IL6* (5'- AGACAGCCACTCACCTCTTCAG, 3'- TTCTGCCAGTGCCTCTTTGCTG) and *IFNA* (5'- GTRACTGCAGAATCTCTCCTTTCTCCTG, 3'- GTGTCTAGATCTGACAACCTCCCAGGCACA). Each sample was assayed in replicates of three, per primer set. Threshold values (C_T) were averaged over each sample replicated, followed by normalization via the $\Delta\Delta C_T$ method to the β -actin housekeeping gene.

***In vivo* IL6 production and the NZB/W F1 murine model of lupus**

10-week old female wild-type (*Irf5*^{+/+}) Balb/c mice (Jackson Laboratories, Bar Harbor, Maine, USA) were either mock-injected with PBS or injected once *i.p.* with 200 µg/mouse of N5-1 in PBS. 1 h later, animals were *i.p.* injected with 100 µg/mouse R848. Age- and gender-matched *Irf5*^{+/-} and *Irf5*^{-/-} Balb/c littermate mice were also injected *i.p.* with R848. 1.5 h post-R848

challenge, blood was harvested and serum isolated for IL6 ELISA (Cayman Chemical, #583371). 7 week-old NZB/W F1 female mice, purchased from Jackson Laboratories, were acclimated for 1 week prior to being IP-injected with PBS or N5-1 at a dose of 100 µg/mouse/injection on Day 0, Day 1, Day 4, Day 7 and Day 14. Body weight was monitored on a daily basis. Immune cell subsets and Irf5 nuclear translocation were analyzed in blood over the course of disease by imaging flow cytometry and/or traditional flow cytometry using antibodies listed in **Supplemental Table 3**. Proteinuria was measured by Bradford protein assay (Bio-rad). Measurement of urine (QuantiChrom Creatinine Assay Kit, BioAssay Systems) and serum creatinine (4000 QTRAP Mass Spectrometer) levels in blinded samples was done at the Animal Physiology and Phenotyping Core at Yale School of Medicine. Serum auto-antibodies (1:100 dilution in PBS) were measured by ANA-HEp-2 (Bio-rad). Images were taken on a Zeiss Apotome microscope, at the same exposure time and magnification (200X). Each image was read blindly and assigned an arbitrary score of 0-4; 0 represents a negative signal and 4 represents the strongest signal. Anti-dsDNA IgG was quantified by ELISA (Alpha Diagnostic International, San Antonio, TX). For kidney pathology, mice were euthanized at 33-37 weeks of age and kidneys harvested for H&E and PAS staining. Multiple sections were examined in a blinded manner for indications of inflammation and tissue damage as described previously (90). Briefly, 100 glomeruli from each case were evaluated. Quantification was based on a 0-4 scale in which the grades 1, 2, 3 and 4 were accorded when 10%, 11-25%, 26-50% and > 50% of the glomeruli were affected, respectively. Images were taken on a Zeiss Apotome at 40X magnification or generated by HistoWiz at 10X magnification.

dsDNA IgG isotype ELISA in MRL/lpr and pristane-induced mice

Female 5-6 week-old MRL/lpr mice were purchased from Jackson Laboratories and acclimated for 1 week prior to testing for serum ANA and Irf5 cellular activation. Positive ANA was uniformly confirmed at 8 weeks-old and mice were randomly assigned to begin the two-week PBS and N5-1 treatment regimen (**Fig. 7B**). Similarly, female wild-type or *Irf5*^{-/-} Balb/c mice (Jackson Laboratories) were injected once *i.p.* with 0.5 ml pristane at the age of 8 weeks (21,47) and ANA monitored weekly. Once ANA was positive, mice were randomly assigned to PBS and N5-1 treatment groups. All pristane-induced mice were treated between the age of 13-18 weeks-old (**Fig. 7I**). Proteinuria was measured by reagent strips using Multistix[®] 5 (Siemens); 1=30mg/dL, 2=100mg/dL, 3=300mg/dL and 4=>2000mg/dL. For anti-dsDNA IgG isotype ELISA, Immulon 2 HB plates (Thermo Fischer Scientific, Cat# 3455) were coated with UltraPure™ Salmon Sperm DNA Solution (Invitrogen, Cat: 15632011) according to the Reacti-Bind DNA Coating Solution (Thermoscientific, Cat# 17250) protocol. Nonspecific binding was blocked with 1% BSA in HBSS for 1 h and serum samples incubated for an additional 1 h. After washing, plates were incubated with AP-conjugated goat anti-mouse IgG, IgG1, IgG2a, IgG3, or IgM (Southern Biotech) for 1 h. After washing, PNPP Substrate (Thermo Scientific Pierce, Cat: 34045) was added and the plates read at 450 nm with Neo2 (BioTek).

IRF5 Homology Model

The human IRF5 V5 sequence was obtained from UniProtKB (Entry ID: Q13568). A homology model of the IRF5 C-terminal inactive monomer IAD and N-terminal DBD was produced by alignment with the IRF3 crystal structure (PDB: 1QWT) followed by three-dimensional model building and energy minimization using Molecular Operation Environment (MOE 2015.10, Chemical Computing Group Inc., Canada). A database of 10 distinct protein models was generated

and showed good overall alignment with the α -carbon backbone of IRF3 template (rms deviation from 0.55 – 0.64 Å). The phi/psi backbone angles and side chain rotamers were evaluated to discard structures with high-energy and disallowed bonds, and the best model was selected for docking studies.

Peptide Docking and MM-GBSA Refined scoring

The inactive IRF5 monomer model obtained from homology modeling was used as the receptor for peptide docking using the peptide docking program within the Schrodinger suite (Bioluminate, Schrodinger, LLC, New York, NY, 2016). The protein receptor region was defined by centroid of the entire IRF5 model. The dimensions of the peptide docking box were set to fully accommodate linear peptides of 15 residues. The N5-1 peptide was constructed and submitted for docking. 10 poses were generated for each independent docking run and ranked by molecular mechanics generalized born surface area (MM-GBSA) refined score (**Supplemental Fig. 2B, Supplemental Table 2**). The top ranking pose with the lowest MM-GBSA ΔG binding energy (-111.087 kcal/mol) is displayed in **Fig. 3A**.

Supplemental References

85. Gladman DD, Ibanez D, and Urowitz MB. Systemic lupus erythematosus disease activity index 2000. *J Rheumatol.* 2002;29(2):288-91.
86. Doucey MA, Goffin L, Naeher D, Michielin O, Baumgartner P, Guillaume P, Palmer E, and Luescher IF. CD3 delta establishes a functional link between the T cell receptor and CD8. *J Biol Chem.* 2003;278(5):3257-64.
87. Barbato C, Canu N, Zambrano N, Serafino A, Minopoli G, Ciotti MT, Amadoro G, Russo T, and Calissano P. Interaction of Tau with Fe65 links tau to APP. *Neurobiol Dis.*

2005;18(2):399-408.

88. Poole E, Strappe P, Mok HP, Hicks R, and Lever AM. HIV-1 Gag-RNA interaction occurs at a perinuclear/centrosomal site; analysis by confocal microscopy and FRET. *Traffic*. 2005;6(9):741-55.
89. Li D, De S, Li D, Song S, Matta B, and Barnes BJ. Specific detection of interferon regulatory factor 5 (IRF5): A case of antibody inequality. *Sci Rep*. 2016;6(31002).
90. Giles BM, Tchepelova SN, Kachinski JJ, Ruff K, Croker BP, Morel L, and Boackle SA. Augmentation of NZB autoimmune phenotypes by the Sle1c murine lupus susceptibility interval. *J Immunol*. 2007;178(7):4667-75.

Supplemental Tables

Supplemental Table 1: IRF5 peptide inhibitor sequences, charge distribution and hydrophobicity[‡].

| Peptide Inhibitor | Sequence | Charge |
|----------------------|--------------------------------|-------------|
| PTD | DRQIKIWFQNRRMKWKK | positive |
| N5-1 | DRQIKIWFQNRRMKWKKPRRVRLK | positive |
| N5-2 | DRQIKIWFQNRRMKWKKRHATRHG | positive |
| N5-3 | DRQIKIWFQNRRMKWKKKSRLF | +/- |
| N5-4 | DRQIKIWFQNRRMKWKKGPRDMPP | hydrophobic |
| N5-5 | DRQIKIWFQNRRMKWKKEGVDEAD | negative |
| C5-2 | DRQIKIWFQNRRMKWKKPREKKLI | +/- |
| FITC-PTD | FITC- DRQIKIWFQNRRMKWKK | SAA |
| FITC-N5-1 | FITC- DRQIKIWFQNRRMKWKKPRRVRLK | SAA |
| FITC-C5-2 | FITC- DRQIKIWFQNRRMKWKKPREKKLI | SAA |
| Non-specific control | DWEYS | negative |

[‡]blue, positively charged; red, negatively charged; green, hydrophobic; purple, special cases.
SAA – same as above.

Supplemental Table 2: Docking score and MMGBSA refined binding energy of the N5-1 peptide on inactive IRF5.

| Pose # | Docking Score | MMGBSA $\Delta G_{\text{Binding}}$ (kcal/mol) |
|--------|---------------|--|
| 1 | -9.303 | -86.130 |
| 2 | -8.985 | -111.087 |
| 3 | -8.840 | -88.498 |
| 4 | -8.820 | -87.095 |
| 5 | -8.698 | -76.134 |
| 6 | -8.636 | -87.094 |
| 7 | -8.592 | -87.349 |
| 8 | -8.308 | -84.659 |
| 9 | -8.269 | -84.889 |
| 10 | -8.238 | -81.170 |

Supplemental Table 3: Antibodies used for flow cytometry analysis of murine cells.

| Anti | Color | Company | Catalog # |
|-------------|--------------|-----------------|------------------|
| CD3 | PE-Cy7 | BioLegend | 100220 |
| CD4 | FITC | BioLegend | 100406 |
| CD8 | PE | BioLegend | 100708 |
| CD11b | PE | BioLegend | 101208 |
| CD11b | Pac Blue | BioLegend | 101223 |
| CD11c | PE | BioLegend | 117308 |
| CD138 | PerCP-Cy5.5 | BioLegend | 142510 |
| B220 | FITC | BioLegend | 103206 |
| B220 | APC | BioLegend | 103212 |
| IgD | AF700 | BioLegend | 405730 |
| Ig | FITC | SouthernBiotech | 1010-02 |
| IgG | FITC | BioLegend | 405305 |
| IRF5 | APC or FITC | Abcam | 181553 |
| IgG(H+L) | APC | Invitrogen | A10931 |
| BD Fc block | | BD Bioscience | 553141 |

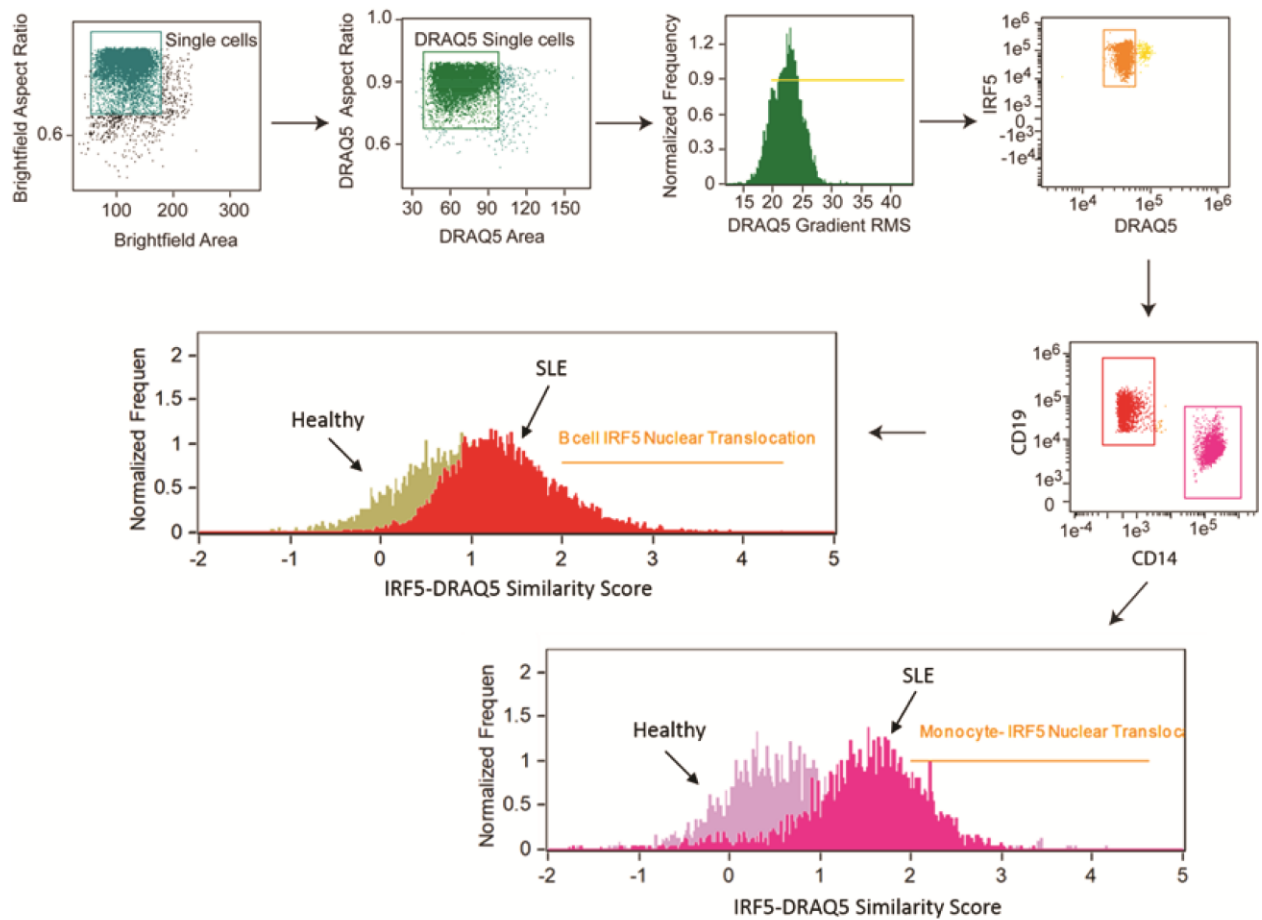


Fig. S1. Representative gating scheme for imaging flow cytometry analysis of IRF5 nuclear translocation. Gating scheme used for determining levels of human IRF5 nuclear translocation in different populations of immune cells by imaging flow cytometry.

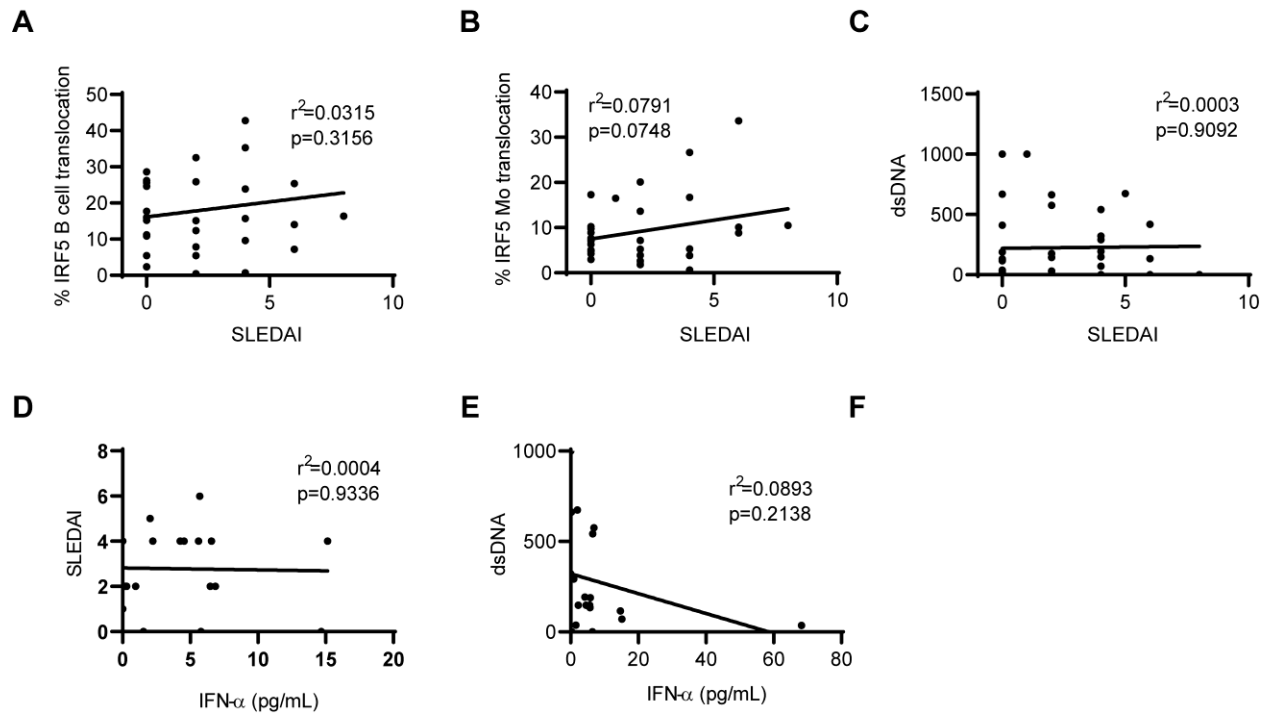


Fig. S2. Correlations between IRF5 hyper-activation, SLEDAI, dsDNA titers and IFN α in SLE patients. Linear regression analyses are shown from data in **Fig. 1C-K**. (**A,B**) Correlation between % IRF5 B cell (**A**) or Mo (**B**) translocation and SLEDAI. (**C**) Correlation between dsDNA titers and SLEDAI. (**D,E**) Correlation between SLEDAI (**D**) or dsDNA titer (**E**) and IFN α .

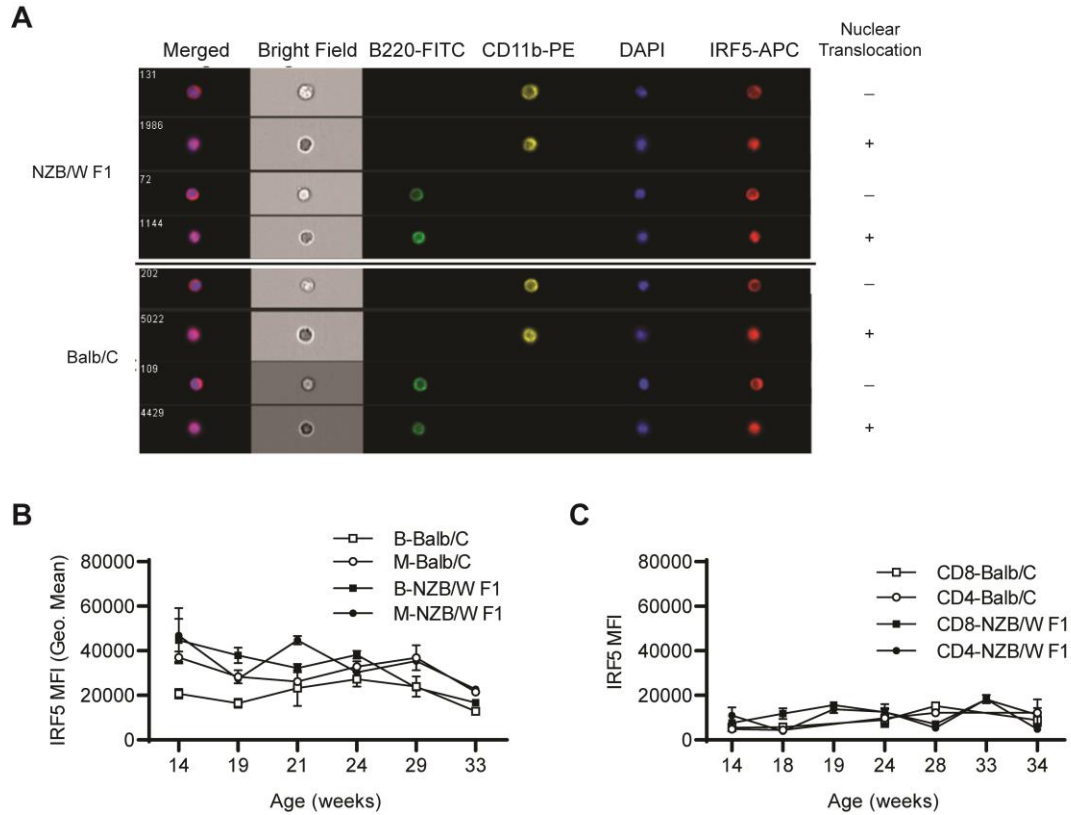


Fig. S3. Tracking murine *Irf5* activation in immune cells from NZB/W F1 mice. (A) Representative images of *Irf5* cellular localization in B220⁺ B cells and CD11b⁺ Mo from age-matched female NZB/W F1 and wild-type Balb/c mice using imaging flow cytometry with similar gating strategies as shown in **Fig. S1**. (B) Total *Irf5* protein expression in monocytes (M) and B cells (B) was plotted as mean fluorescence intensity (MFI) from imaging flow data in **Fig. 1L-Q**. Expression changes are shown over time in aging mice. (C) Same as (B) except *Irf5* expression changes are shown in CD4⁺ and CD8⁺ T cells from NZB/W F1 and Balb/c mice. These data correspond to data in **Fig. 1R-S**. *n* = 6 mice per group. All values reported as means ± SEM.

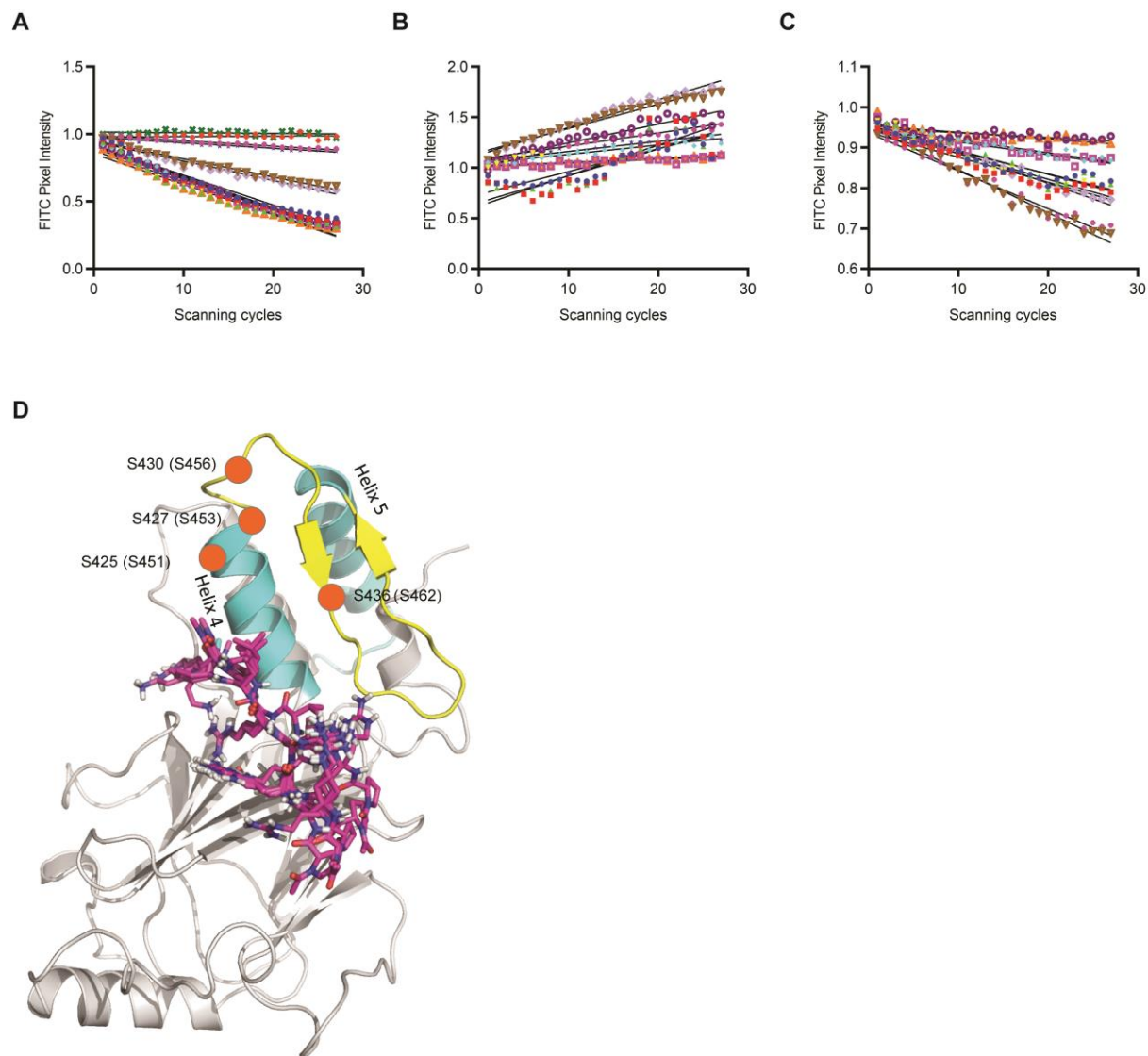


Fig. S4. N5-1 selectively binds to IRF5 and not IRF3 or IRF7. (A-C) Linear regression lines from Fig. 2H of ratio of FITC pixel intensity as compared to baseline intensity for a representative set of IRF3 (A), IRF5 (B) and IRF7 (C) cellular analyses. Data from 15 cells per antibody were captured; each line represents one cell. (D) Docking of N5-1 to IRF5. Similar to Fig. 3A, this schematic diagram shows the top ten N5-1 docking poses on the C-terminal IAD of an inactive IRF5 monomer. Docking poses are from docking score and MM-GBSA refined binding energies listed in ST2. N5-1 is shown in pink, serine phosphorylation sites are shown by orange circles.

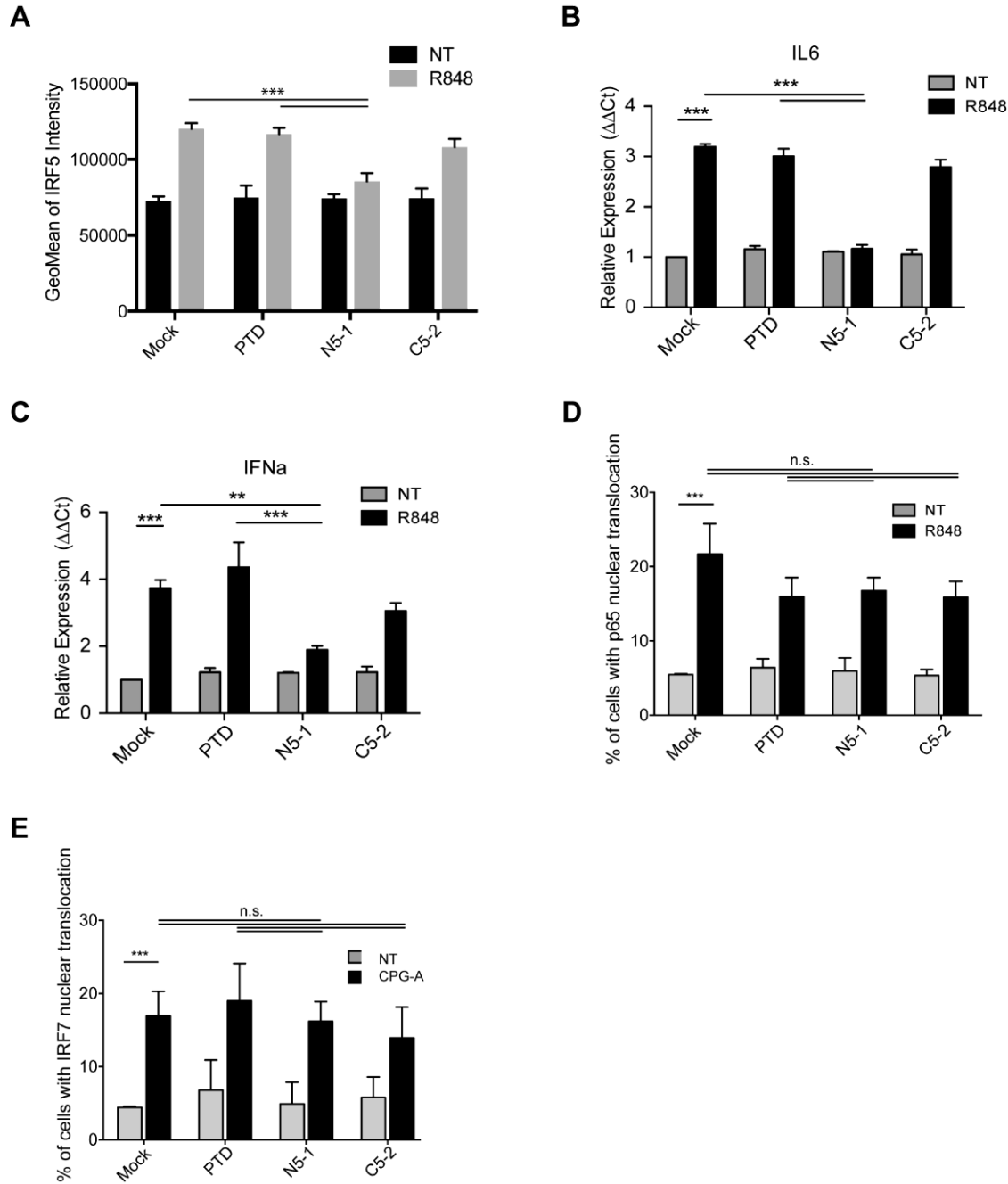


Fig. S6. Impact on cytokine expression and specificity for NFκB or IRF7. (A) PBMC were treated with 10 μM inhibitor for 1 h and surface-stained for CD14⁺ Mo. After fixation, cells were permeabilized and stained for intracellular IRF5. GeoMean of IRF5 intensity from imaging flow cytometry is shown; *n* = 3 healthy donors. (B and C) Relative expression of *IL6* (B) and *IFNA* (C) in primary PBMC pre-incubated with either mock, 10 μM PTD, N5-1, or C5-2 and stimulated with R848; *n* = 4 healthy donors. (D) Percentage of Mo with p65 nuclear translocation following 1 h pre-incubation with 10 μM inhibitor and R848 stimulation for 30 mins; *n* = 4 independent healthy

donors. (E) Percentage of pDCs with nuclear IRF7 following 1 h pre-incubation with 10 μ M inhibitor and CpG-A stimulation for 2 h; $n = 4$ healthy donors. Statistical significance was determined by two-way ANOVA. All values reported as means \pm SEM. ** $p < 0.01$, *** $p < 0.001$.

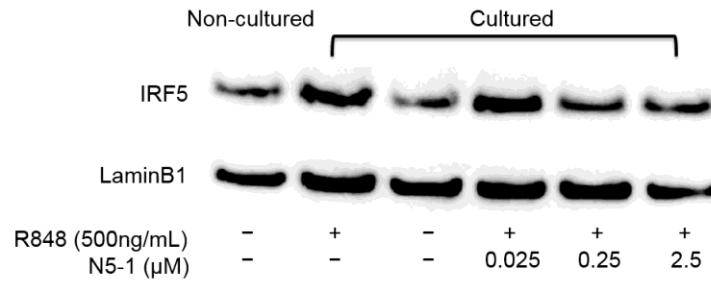


Fig. S7. N5-1 inhibits R848-induced murine Irf5 nuclear translocation. RAW264.7 macrophages were fractionated into nuclear extracts following 1 h pre-treatment with N5-1 and stimulation with 500 ng/mL R848 for 2 h. Non-cultured cells represent time 0 h before pre-treatment; cultured cells are after 3 h incubation. Representative Western blot of nuclear fractions is shown.

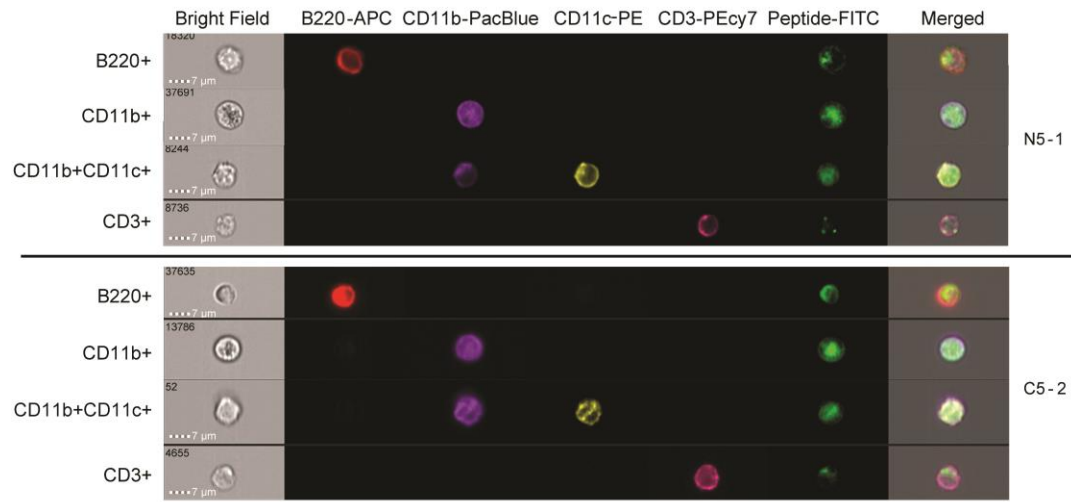
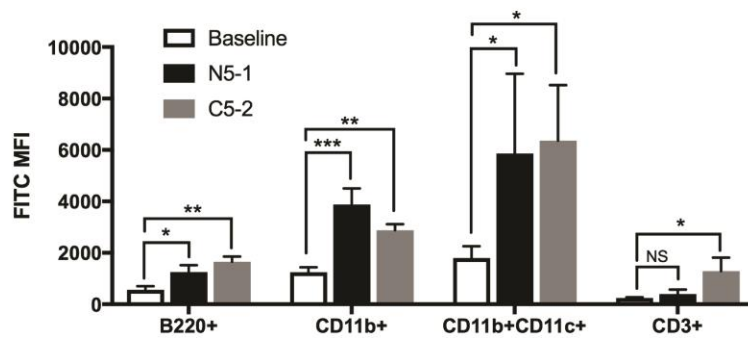
A**B**

Fig. S8. *In vivo* cellular uptake of inhibitors in NZB/W F1 mice. (A) Representative images showing cellular uptake (in B cells - B220⁺, Mo - CD11b⁺, DC - CD11b⁺CD11c⁺ and T cells - CD3⁺) of FITC-conjugated N5-1 or C5-2 at 2h post-injection by imaging flow cytometry. 60X magnification. (B) Summarized data from (A) showing FITC mean fluorescence intensity (MFI) of each inhibitor in each cell type. $n = 3$ mice per treatment group. Statistical significance was determined by one-way ANOVA. Values reported as means \pm SEM. * $p < 0.05$, ** $p < 0.01$, *** $p < 0.001$, NS - not significant.

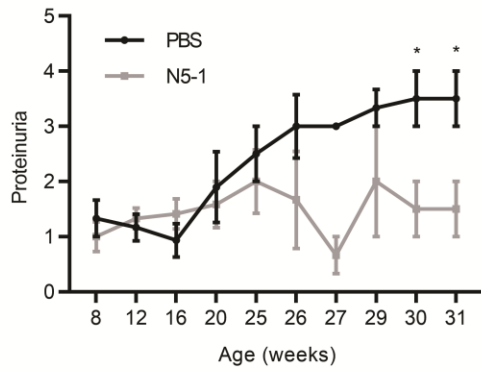
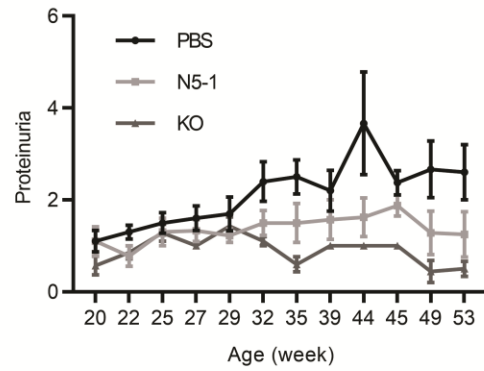
A**B**

Fig. S10. Proteinuria in PBS- and N5-1-treated MRL/lpr and pristane-induced lupus mice. (A) Urine protein levels were measured weekly in PBS- or N5-1-treated MRL/lpr mice. Black circles denote PBS-treated mice and light grey circles denote N5-1-treated mice. **(B)** Same as (A) except pristane-injected PBS- or N5-1-treated wild-type or *Irf5*^{-/-} (KO) Balb/c mice were monitored. Black circles denote PBS-treated mice; light grey circles denote N5-1-treated mice; dark grey circles denote KO mice. $n = 6$ mice per treatment group. Differences between age-groups determined by multiple t test, * $p < 0.05$ vs. N5-1, FDR < 0.05 .

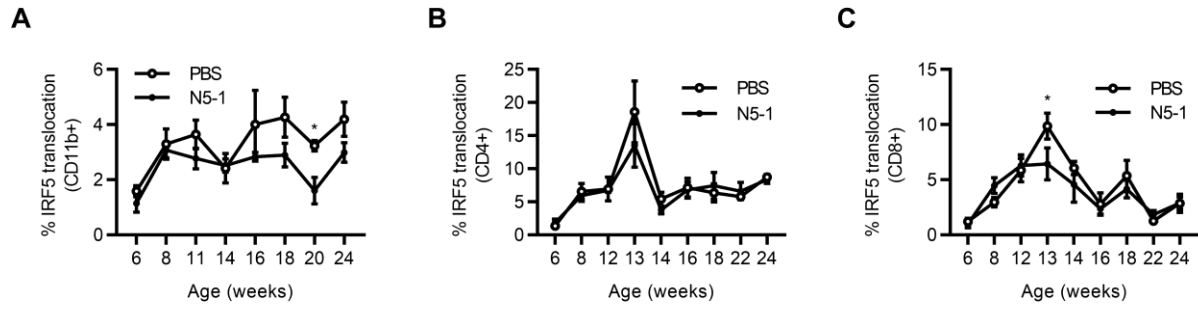
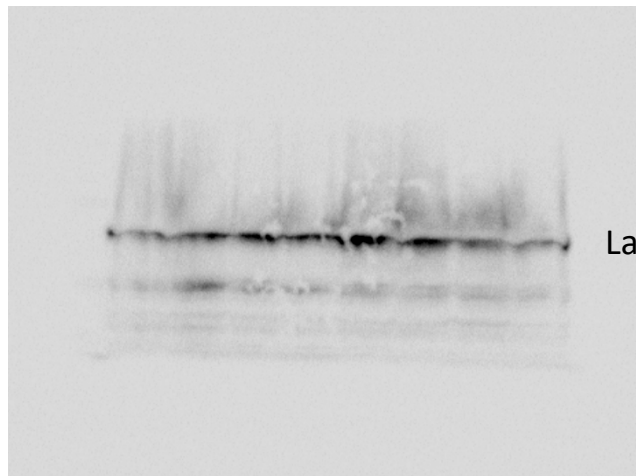
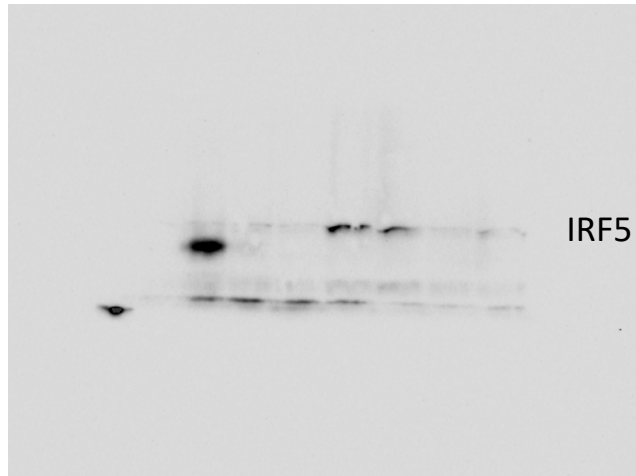
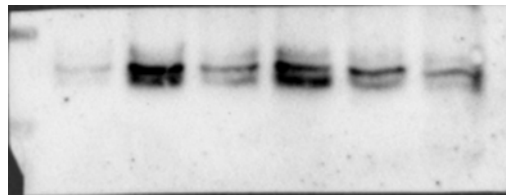
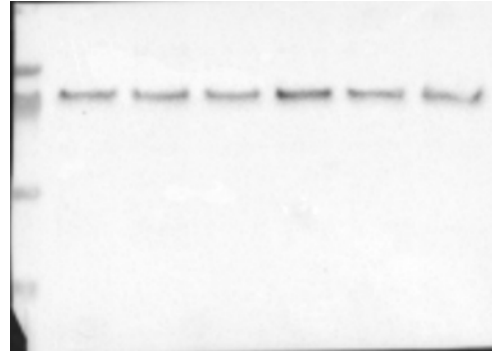


Fig. S11. Tracking of *Irf5* cellular activation in MRL/*lpr* mice. (A-C) Analysis of *Irf5* nuclear translocation in CD11b⁺ Mo (A), CD3⁺CD4⁺ T cells (B) and CD3⁺CD8⁺ T cells (C) from aging female MRL/*lpr* mice. *n* = 4 mice per group. Statistical significance was determined using two-way ANOVA with a Bonferroni post hoc test. All values reported as means ± SEM. *(*p* ≤ 0.05).

Full unedited gel for Figure 4G



Full unedited gel for Figure 5A



Full unedited gel for Suppl. Figure 7

